

**The Effect on Alkali Metal (Na and K) doping on Thermo-chromic Properties of VO<sub>2</sub> films by Sol-gel Spin Coating on Glass**

Işıl Top<sup>a\*</sup>, JohannesSchläfer<sup>b</sup>, Ioannis Papakonstantinou<sup>b</sup>, Sriluxmi Srimuruganathan<sup>a</sup>, Michael Powell<sup>c</sup>, Claire J Carmalt<sup>c</sup>, Russell Binions<sup>a+</sup> Isaac and Isaac Abrahams<sup>d\*</sup>

a: School of Engineering and Materials Science, Queen Mary University of London,  
Mile End Road, E1 4NS, UK

b: Department of Electronic and Electrical Engineering, University College London,  
Torrington Place, WC1E 7JE, UK

c: Department of Chemistry, University College London, 20 Gordon Street, London.  
WC1H 0AJ, UK.

d: School of Biochemical Sciences, Queen Mary University of London, Mile End Road,  
E1 4NS,UK

\*Corresponding authors: i.top@qmul.ac.uk

\*i.abrahams@qmul.ac.uk

<sup>+</sup> deceased

## **Abstract**

This work reports thermochromic thin films based on alkali metal doped VO<sub>2</sub>, produced by sol-gel spin coating at 450 °C. The effect of sodium and potassium on the thermochromic transition temperature as well as solar modulations were investigated. The dopant amount was 1.5 % for both. Both sodium and potassium resulted in a reduction of critical transition temperature ( $T_c$ ) from 62 °C to 57 °C and 57 °C respectively. Similarly, both dopants improved the solar modulations ( $T_{sol}$ ) of the undoped VO<sub>2</sub> films from 3.81 to 9.44 and 5.43, respectively. The significance of achieving thermochromic switching response at temperatures 450 °C by a sol-gel with incorporation of alkali metal ion source is highlighted.

## **Keywords**

Vanadium dioxide, thermochromics, doping, chromogenics, sol-gel

## **1. Introduction**

Energy efficient windows refer to windows which can intelligently control the amount of light and heat passing through, when triggered by an external stimulus such as voltage (electrochromic), temperature (thermochromic), UV illumination (photochromic) and reductive or oxidizing gases (gasochromic). Vanadium oxides exhibit thermochromic properties, among which VO, V<sub>2</sub>O<sub>3</sub>, VO<sub>2</sub> and V<sub>2</sub>O<sub>5</sub> undergo metal–insulator phase transitions at the critical temperatures ( $T_c$ ) of 126 K (-147.15 °C) , 150 K (-123 °C)<sup>1</sup>, 341 K (68 °C)<sup>2</sup> and 553 K (280 °C)<sup>3</sup>, respectively. Among other vanadium oxides, VO<sub>2</sub> has received much of interest in recent years, due to potential application as solar control coatings. Since buildings account for ~40% of the total world energy consumption, this is primarily due to heating and cooling demands, and most of the energy loss occurs through windows, VO<sub>2</sub> coatings on windows can be used to reduce these energy demands<sup>4</sup>. This reduction in the energy

consumption would lead a lower greenhouse gas emissions, allowing humanity to achieve Paris agreement to limit human-induced climate change to less than 2 °C above pre-industrial levels.

The thermochromic smart window technology is based on a temperature induced fully reversible structural phase change from the higher temperature tetragonal rutile structure to lower temperature monoclinic structure<sup>5</sup>. A remarkable feature of the monoclinic phase is the presence of V-V pairs along its *a* axis. During this first order phase transition, the tetragonal rutile form transforms to an alternate V-V separation, resulting in small lattice distortion along the *c* axis, leading to pairing of vanadium atoms and a distinct band structure in each phase<sup>6</sup>. In the monoclinic phase (for temperatures below  $T_c$ ), the material is transparent to both UV-Vis and NIR irradiation, therefore the solar radiation and associated heat will reach to the interior of the building. On the other hand, upon passing through the  $T_c$ , the material becomes highly reflective of near IR wavelengths whilst still being transparent to visible wavelengths. By this way, the heat gain from solar radiation will be high in winter and much lower in the summer, reducing the buildings energy demands in heating and cooling, respectively. For optimal energy efficiency VO<sub>2</sub> solar control coatings ideally should be transparent in the UV-Vis region whilst displaying a large change in optical properties in near IR wavelengths. Furthermore, there should be no significant change in the visible light transmittance observed upon going through the phase transition<sup>7</sup>. The thermochromic performance is characterised by  $\Delta T$ , the percent transmittance modulation between cold and hot stages (Equation. 1)<sup>8</sup>. Wavelength integrated luminous and solar transmittance values are expressed in equation (3), where  $\tau$  indicates the thickness of VO<sub>2</sub> thin film,  $\phi$  is the spectral sensitivity of the light adapted eye and  $\lambda$  the wavelength of light.<sup>9</sup> These integrated values allow an assessment for visual and energy-related performance of the thermochromic thin films.

$$DT(\%) = T_{\text{coloured}} - T_{\text{transparent}} \quad (1)$$

$$T_{\text{lum,sol}}(\tau) = \frac{\int d\lambda \varphi_{\text{lum,sol}}(\lambda) T(\lambda, \tau)}{\int d\lambda \varphi_{\text{lum,sol}}(\lambda)} \quad (2)$$

In all glazing systems visible transmittance of at least 60 % is desirable so as to allow enough light to the building. High quality solar control coatings should show abrupt change in near IR optical properties when they switch between the transmissive and reflective states. However in practise this doesn't exist, and the requirement for noticeable solar energy modulation limits  $\Delta T_{\text{lum}}$  to 40%, and the modulation of  $\Delta T_{\text{sol}}$  does not exceed 10% <sup>10</sup>. Furthermore, the transition temperature of these materials will need to be reduced from *ca.* 68 °C, for typical undoped VO<sub>2</sub> materials, to temperatures between 20 and 25 °C, in order to maximise the time the coating spends in the higher temperature state and thus decrease the need for air conditioning <sup>11</sup>. There have been several approaches reported to lower the  $T_c$  of VO<sub>2</sub> materials. The majority of these studies have looked at the doping films with high valence transition metals such as W, Nb and Mo. Epitaxial growth has also been shown to reduce the  $T_c$  through the promotion of strain <sup>12</sup>. It has been suggested that doping with high valence transition metals reduces the  $T_c$  through the injection of electrons into the V 3d valence bands, this destabilises the V–V pairs, promoting the tetragonal VO<sub>2</sub>(R) phase and so lowering the energy required for the phase transition <sup>13</sup>.

Tungsten has been found to be the most efficient dopant, lowering  $T_c$  by 19 °C <sup>14</sup>, 20-25 °C <sup>15</sup> and 31 °C per at % <sup>16</sup>. Molybdenum doping has also been explored and found to decrease by 7 °C <sup>17</sup> and 15 °C <sup>18</sup> per at % doping. Doping with 3 mol % Mo decreased the  $T_c$  to 42 °C <sup>19</sup>. Another promising reduction in the  $T_c$  was obtained by using fluorine, which reduced  $T_c$  to 35 °C by 3 at % <sup>20</sup>. Other dopants explored include niobium, magnesium and cerium which decreased  $T_c$  typically 3 °C <sup>21</sup> and 4.5 °C <sup>22</sup> by 27 °C % <sup>12</sup>, respectively per at % doping. Gold was also explored because of its surface plasmon resonance that is strongly

absorbing. It found to be an effective dopant to reduce the  $T_c$  by 18 °C with 1 at % dopant incorporation; however it affected the thermochromic efficiency in a detrimental manner, by resulting in a significant hysteresis loop width <sup>5</sup>.

There has been very little literature published on alkali metal or alkali earth metal doping to reduce the phase transition temperature in VO<sub>2</sub> thermochromic materials. Alkali earth metal doping of VO<sub>2</sub> with and  $T_c$  decreased by -0.6, -0.5, 0.4, and -0.6 K/at. % for Ba, Ca, Mg, and Sr, respectively <sup>23</sup>. Alkali earth dopants were reported by calculation based studies as well. For instance Be doping were shown to change the electronic structure by injecting additional electrons which reduce the transition temperature by 58 K (-215.15) per at % Be <sup>24</sup>. However, Be is very toxic, therefore it is not a good and environmentally-friendly dopant source. Sodium was used as co-dopant to W doped VO<sub>2</sub> films, and with the assistance of sodium, doping with tungsten (1 at % Na<sub>2</sub>WO<sub>4</sub>) yielded an extra depression in phase temperature of 6–12 °C over that of 20–26 °C per at % of tungsten itself<sup>25</sup>. Li, Na and K dopants were also investigated by calculation and K found to effectively decrease the  $T_c$  as well as improve the transmittance modulation in near infra-red region. Level of 1 at % could reduce the phase transition temperature of VO<sub>2</sub> by 43 K, 49 K, 94 K, respectively <sup>26</sup>. To the best of our knowledge, these dopants have not been reported in any experimental work yet. Therefore, motivated by this study, we herein employ experimental work to deposit VO<sub>2</sub> films doped with Na and K to modulate the transition temperature.

## **2. Experimental**

### **2.1. Thin Film Preparation**

In this work, undoped and Na and K doped VO<sub>2</sub> films were fabricated by sol-gel spin coating followed by a subsequent annealing step<sup>27</sup>. Firstly, 5.2 ml vanadium oxytriisopropoxide (Aldrich, 98 %) was dissolved in 69 ml isopropanol (Sigma-Aldrich, 98%), under constant stirring. Then, 0.61 ml of acetyl acetone (VWR Chemicals, 99 %) was

added dropwise to this solution, and the solution was stirred for 15 min. Following, 6.86 ml of acetic acid (Sigma-Aldrich, 99.8 %) was added dropwise, and left for stirring 15 more min. Finally, in order to prepare the doped solutions, sodium acetate and potassium acetate (Sigma-Aldrich, 99,9 %) were added separately to the VO<sub>2</sub> sol. The amount of dopants incorporated was set to 1.5 wt. % in order to achieve best thermochromic switching response and shown in Table 1. The solutions were left for aging overnight.

From these solutions, VO<sub>2</sub> coatings were produced by sol-gel spin coating and subsequent annealing. Prior to the spin coating, silica coated glass substrates provided by Pilkington were cut into 2 cm x 2 cm, and washed with soap, water, acetone, isopropanol, left to ultrasonic bath for 20 minutes and dried under N<sub>2</sub> flow to ensure completely clean substrates. Spin coating was carried firstly for 500 rpm for 5 sec, and 3000 rpm for 40 sec in order to get optimal spin coating conditions. 5 layers of VO<sub>2</sub> was coated. Subsequently, the as-deposited films were annealed at 450 °C for 15 min with a heating rate of 10 °C min<sup>-1</sup>. The annealing was carried out under 5% H<sub>2</sub>- 95% N<sub>2</sub> environment with a gas flow rate of 1 L min<sup>-1</sup>.

**Table 1.** Tabulation of sample names and preparation conditions.

<b>Dopant Name</b>	<b>Dopant percent (wt. %)</b>	<b>Annealin g Temperature (°C)</b>	<b>Annealin g Duration (min)</b>	<b>H<sub>2</sub>-N<sub>2</sub> Gas Flow Rate</b>	<b>Substrate</b>
-	0	450	15	1	Silica coated glass
Na	1.5	450	15	1	Silica coated glass

K	1.5	450	15	1	Silica coated glass
---	-----	-----	----	---	------------------------

## 2.2. Characterisation

### 2.2.1. General Characterisation

Scanning electron microscopy (SEM) investigations were carried out to analyse the crystallite surface structure of the synthesized coatings, by an *FEI Inspect F Field Emission SEM* at an accelerating voltage of 10 keV and spot size of 3 nm and a working distance of 10 mm. Prior to SEM measurements, samples were overcoated with a thin film of gold for 60 sec in order to make them more conductive. X-ray diffraction (XRD) measurements were made on a *Panalytical X'Pert Pro* diffractometer fitted with an *X'Celerator* detector in glancing angle ( $\alpha = 3^\circ$ ) mode, using Ni filtered Cu-K $\alpha$  radiation ( $K\alpha_1 = 1.5405980 \text{ \AA}$  and  $K\alpha_2 = 1.5444260 \text{ \AA}$ ). The diffraction patterns were collected over  $2\theta$  range  $20\text{--}70^\circ$  with a step size of  $0.033^\circ$  and an effective count time of 1.7 s per step.

### 2.2.2. Thermochromic Activity

UV/vis/NIR transmission spectra was measured using a *Perkin-Elmer Lambda 950 UV–Vis–NIR* spectrometer over the wavelength range of  $300\text{--}2500 \text{ nm}$  with an air spectral background. In order to determine the thermochromic properties of the films, transmission was recorded above and below  $T_c$  by heating the samples on a hot plate. Hysteresis data were obtained for films by heating between *ca.*  $20 \text{ }^\circ\text{C}$  and  $80 \text{ }^\circ\text{C}$ , using a custom-built heated sample holder. Spectra were recorded at  $5 \text{ }^\circ\text{C}$  intervals on heating and cooling.  $T_c$  was measured as the mid-point of the hysteresis loop. The hysteresis loops were plotted at  $2500 \text{ nm}$ .

### 2.2.3. XPS:

X-Ray photoelectron spectroscopy was conducted on a *Thermo Scientific K-alpha* spectrometer with monochromated Al K $\alpha$  radiation, a dual beam charge compensation system and constant pass energy of 50 eV (spot size 400  $\mu$ m). Survey scans were collected in the binding energy range 0–1200 eV. High-resolution peaks were used for the principal peaks of V (2p), O (1s), Na (1s), K (2p), Cl (2p) and C (1s). Data was calibrated against C1s (285.0 eV). Data was fitted using CASA XPS software.

#### **2.2.4. Adhesion Tests**

Sample adhesion was tested using the standard Scotch tape test as well as attempted abrasion using tissue paper, and brass and steel styli.

### **3. Results and Discussion**

#### **3.1. Physical Properties of the Films**

All of the VO<sub>2</sub> films produced from sol-gel spin coating method were dark yellow/green, typical of VO<sub>2</sub> films<sup>23</sup>, and upon doping there was no difference observed. All films exhibited a good adherence to the substrate after annealing, they were resistant to brass and steel styli and passed the scotch tape test.

The XRD patterns of typical thin films are shown in Figure 1. In this work, previously higher annealing temperatures of 500, 550 and 600 °C were employed, for 30 min, 1 h and 2 h annealing durations. However, the thermochromic properties were observed at only annealing at 450 °C for 15 min, therefore all films were produced at the lowest annealing temperature. Normally higher temperatures are required to achieve phase pure monoclinic VO<sub>2</sub> films with thermochromic switching response<sup>28</sup>.

The crystalline nature of all films was corroborated by XRD experiments (Figure 1). The bottom XRD pattern belongs to the plain vanadium dioxide film which only gave rise to some weak diffraction peaks which could be assigned to the monoclinic vanadium dioxide phase VO<sub>2</sub>(M) (*P* 2<sub>1</sub>/*c*). The XRD pattern of the sodium-doped film, as shown in the middle, shows

the coexistence of two polymorphs. Beside the peaks which could be assigned to the VO<sub>2</sub>(M) phase, intense diffraction peaks for the monoclinic VO<sub>2</sub>(B) phase could be observed. For the potassium-doped films (is on the top) only peaks for the VO<sub>2</sub>(B) were observed. It is know from experiments on macroscopic crystals that doping with lower valent metal cations could stabilize different polymorphs of VO<sub>2</sub> at room temperature such as VO<sub>2</sub>(M2) and VO<sub>2</sub>(T)<sup>29</sup>. The formation of the VO<sub>2</sub>(B) phase could be explained by the strain induced by the dopant. For example, high amount of tungsten dopant (8. at%) in sol-gel derived VO<sub>2</sub> films was reported to result in the isolation of VO<sub>2</sub>(B) phase<sup>30</sup>.

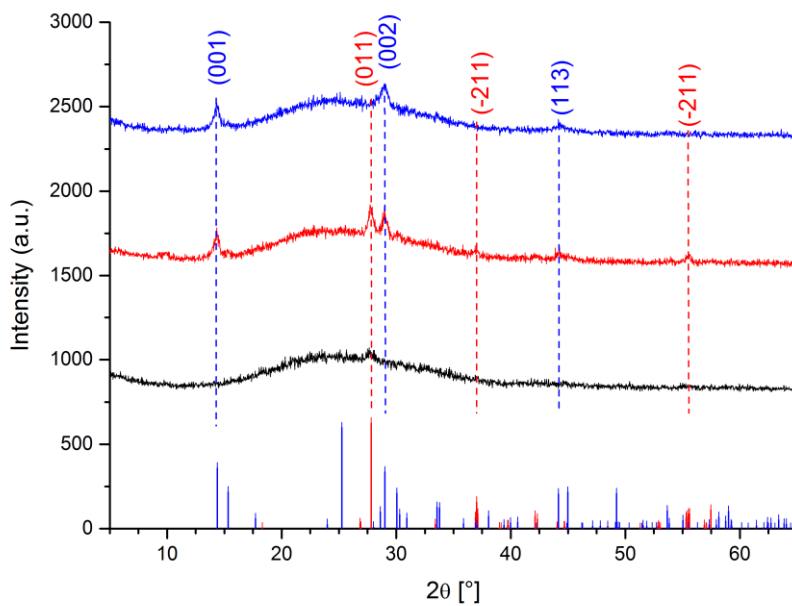


**Figure 1.** XRD plots of undoped, VO<sub>2</sub>, Na and K doped films.

The chemical environments and oxidation state of doped films were investigated by XPS, Figure 2. As shown, for both the Na and K-doped samples, (Figure 2. a and Figure 2. c), the V2p<sub>3/2</sub> environment was deconvoluted to give 3 species, these were at 515.0, 516.1 and 515.7

eV, which corresponded to literature values for  $V^{3+}$ ,  $V^{4+}$  and  $V^{5+}$  respectively ( $\pm 0.2$  eV)<sup>31</sup>. For both samples, the  $V^{3+}$  was a small component of the total environment, with the  $V^{4+}$  and  $V^{5+}$  environments accounting for over 90% of the signal. This  $V^{3+}$  component is attributed to over-reduction by the  $H_2/N_2$  treatment. Furthermore, the K-doped  $VO_2$  sample showed a larger proportion of  $V^{4+}:V^{5+}$  in the XPS spectrum, Figure 2. c). This suggests that this precursor solution could promote the formation of  $V^{4+}$ . The O1s spectra, Figure 2. b) and d), was deconvoluted to give three environments which are attributed to  $VO_x$ , O-C and O-H species<sup>31</sup>. Although the K2p region was scanned, there was no detectable K signal for the K-doped sample. In both the Na and K-doped samples there was a trace amount of Na present, but this was below the reliable detection limit of XPS (1at. %), therefore these are not presented here. This suggests that for both dopant types, there is minimal incorporation into the  $VO_2$  lattice.

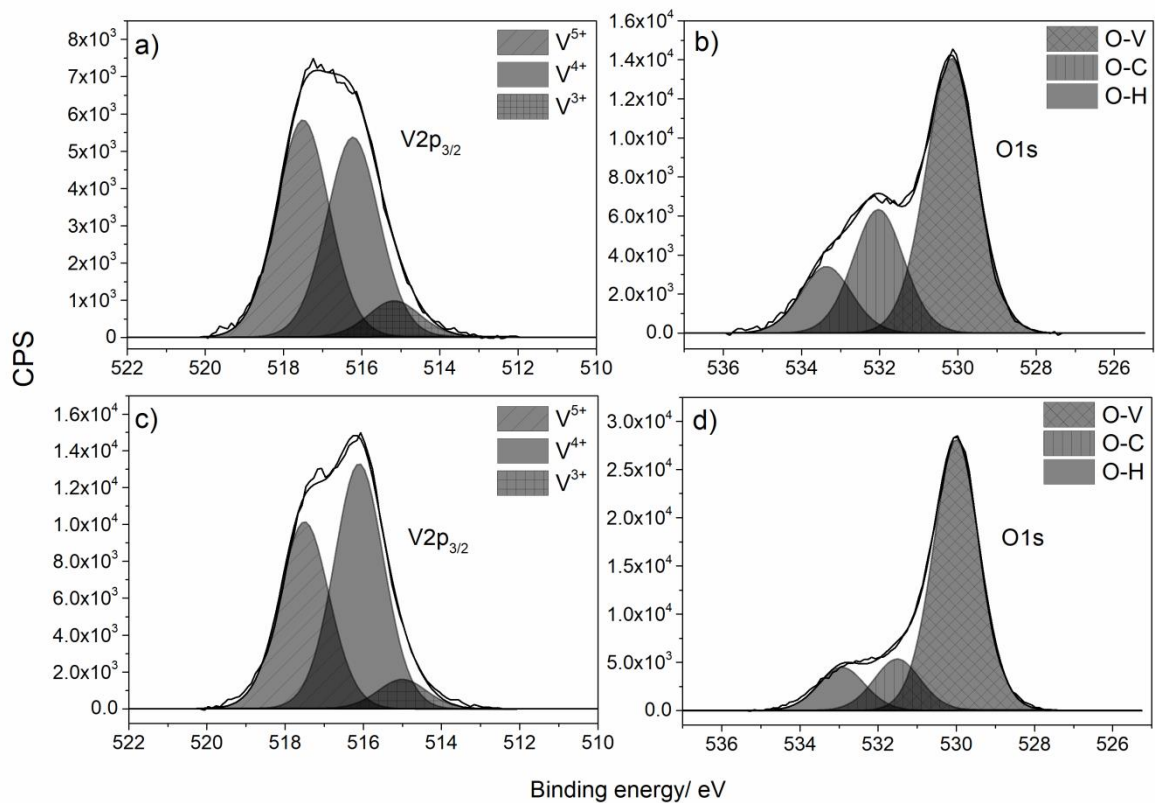


**Figure 2:** Typical XPS spectra for a) and b) Typical  $V2p_{3/2}$  and O1s environments for Na-doped  $VO_2$  sample and c) and d) Typical  $V2p_{3/2}$  and O1s environments for K-doped  $VO_2$  sample.

### 3.2. Surface Morphology of the Films

Figure 2 shows the SEM images of undoped (a), Na (b) and K(c) doped VO<sub>2</sub> films produced by sol-gel spin coating on silica coated glass substrates. The images were obtained at 60,000 x magnification. All three films exhibited a complete surface coverage whereby inclusion of sodium or potassium in solution resulted in a significant change in the surface morphology of the coated films, similar to 1 at. % W doped films previously reported<sup>32</sup>. As shown in the Figure 3. a, the surface of the undoped VO<sub>2</sub> film was comprised of small nanoparticles with average size of ~15 nm, covered evenly the substrate. When it was doped with Na (1.5 wt. %), there was a dramatic change on the microstructure to an irregular and porous morphology, as shown in the Figure 3. b. Compared to the un-doped film, this film consisted islands, and plate-like structures, leaving the surface a porous appearance. The final image (Figure 3.c) belongs to the K doped (1.5 wt. %) VO<sub>2</sub> film. From the image it can be seen that, the surface has a similar morphology to Na doped film, with irregular and porous appearance. However this sample had with smaller particles (50 nm in diameter) coalesced more, and the plate-like structures were less obvious. From these images in can be concluded that, very low amounts of dopants could effectively change the surface morphology to plate like and island formation.

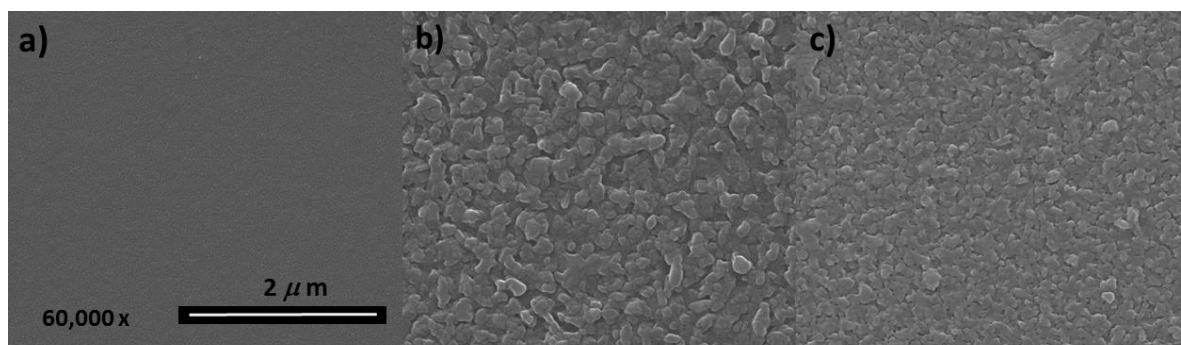


**Figure 3.** SEM images of the a) Undoped, b) Na doped c) and K doped VO<sub>2</sub> films, produced by sol-gel spin coating on silica. All the images were recorded at 60,000 x magnification.

### 3.3. Thermochromic Properties of the Films

Thermochromic properties of the films were measured by UV-Vis-NIR spectroscopy to characterise the transmittance modulation ( $\Delta T$ ) in the NIR region and the critical transition temperature ( $T_c$ ). Figure 4 shows the thermally induced reversible spectral changes in the UV-Vis-NIR transmittance for the studied un-doped and doped VO<sub>2</sub> films between room temperature and 80 °C. It was observed that they all displayed the properties required for thermochromic applications, even they exhibited weak crystallinity, and not confirming a phase purity.

All three films exhibited thermochromic modulation with a decrease in transmittance at 80 °C. The percent transmittance modulation ( $\Delta T$ ), solar and luminous transmittance values ( $T_{sol}$  and  $T_{lum}$ ) as well as critical transition temperatures ( $T_c$ ) were tabulated in the Table 2. The maximum transmittance modulation occurs at 2500 nm, therefore  $\Delta T$  values and hysteresis plots were obtained from the data collected at this wavelength. From the data observed in the Figure 4. a, all the percentage changes in the in the transmittance ( $\Delta T_{2500\text{ nm}}$ )

between cold and hot states was 25 % for the un-doped VO<sub>2</sub> film. This result is in a good agreement with the previous reports<sup>33,34</sup>. Figure 4. b and Figure 4. c belongs to the spectra of potassium and sodium doped VO<sub>2</sub> films, respectively. It can be seen that, both dopants resulted in an increase of the NIR transmittance modulation, with 31 % and 41 % for the K and Na doped films, respectively. The change in the solar modulation  $\Delta T_{\text{sol}}$  is also in a good agreement with  $\Delta T_{2500 \text{ nm}}$ , which is further proved our above mentioned analysis. Undoped VO<sub>2</sub> film has a solar modulation of 3.82, which is either similar<sup>32,35</sup> or slightly less than reports based on sol-gel method<sup>34</sup>. Inclusion of potassium resulted in an increase of the  $T_{\text{sol}}$  to 5.43012. Compared to potassium, sodium resulted in a higher increase of  $T_{\text{sol}}$  to 9.44549, which is comparable to the W doped films previously published<sup>32</sup>.

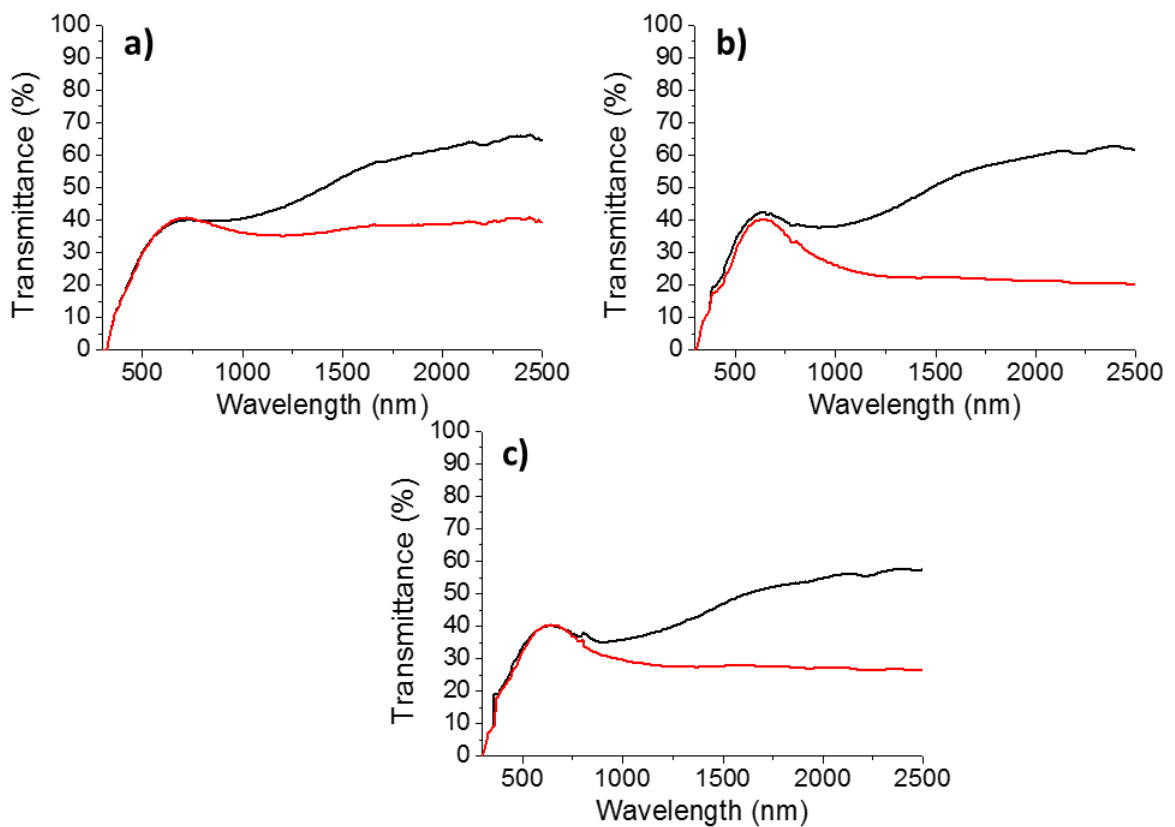


**Figure 4.** Hot and cold UV/Vis/NIR transmittance spectra of a) undoped, b) Na doped and c) K doped VO<sub>2</sub> films produced by sol-gel spin coating on silica glass coated substrates,

annealed at 450 °C for 15 minutes. Black and red lines denote cold and hot states, respectively.

Moreover, the hysteresis loop and the transition temperature of the coatings were studied through the change in transmittance with temperature at 2500 nm as shown in the Figure 5. The black and red lines denote heating and cooling directions, respectively. These values were determined through a plot of  $d(\text{Transmittance})/d(\text{Temperature})$  vs. Temperature, as shown in the Figure 6. Hence, the critical transition temperature ( $T_c$ ) was found to decrease from 62 °C after both dopant incorporations. The first dopant, sodium decreased the  $T_c$  to 57 °C. Compared to Na doping, K dopant was found to be the most efficient one, as it offered a higher  $T_c$  reduction to 47 °C. These values are still higher than as reported by Cui *et al.*<sup>26</sup> who reported first-principle calculations on the basis of sodium and potassium doped VO<sub>2</sub> films, can reduce the  $T_c$  by 49 K and 94 K per 1 at % dopant. Similarly, potassium resulted in a higher degree of reduction in the  $T_c$ , with 15 °C per 1.5 % dopant. Reduction in the  $T_c$  values can be attributed to dopant atoms providing or removing some of the, respectively.  $t_{1/2}$  electrons in the V 3d valence bands, and make some V-V pairs break in monoclinic phase. This brings about destabilisation of VO<sub>2</sub> and hence decreases the  $T_c$ .

Similar to  $T_c$  calculations, From the Figure 6 also shows the hysteresis loop width of the samples. un-doped film was 15 °C, while the  $T_c$  and the hysteresis width of the Na and K doped films were calculated to be 20 °C. From the data, it can be seen that, doping decreases the transition temperature, while having a detrimental effect on the hysteresis loop width. Since the hysteresis width is due to nucleation barriers such as grain boundaries and voids, the microstructure of the coatings, which is different for each sample as evident from SEM images, can affect the width.

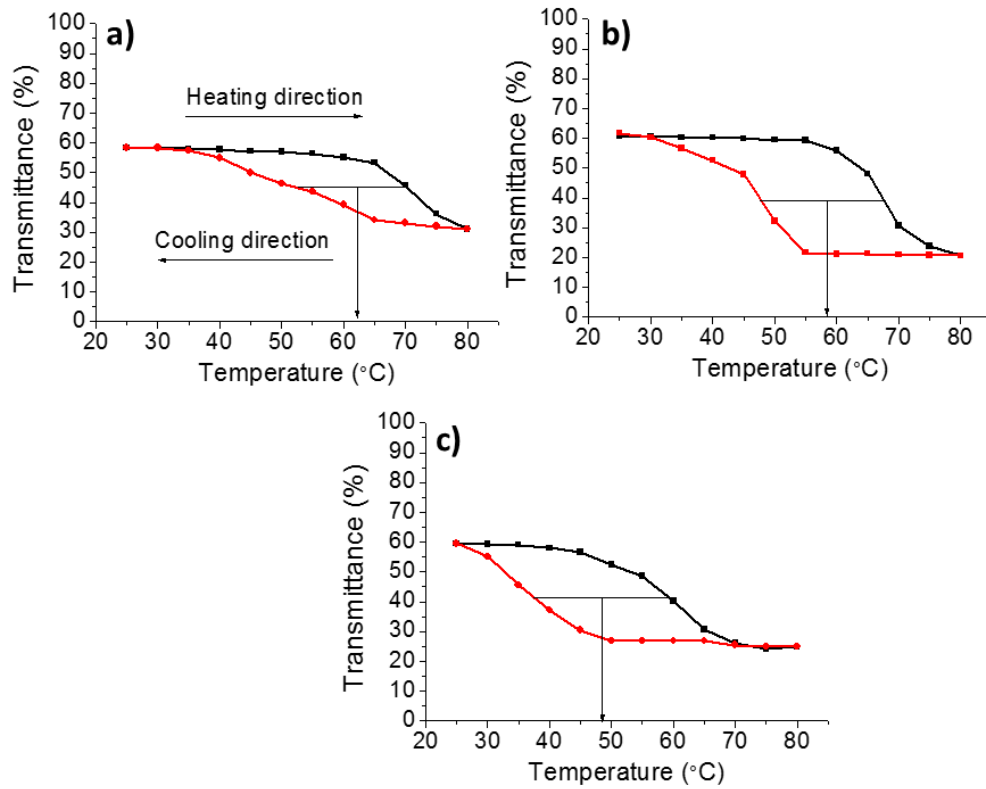


**Figure 5.** Hysteresis plots of plain, Na doped and K doped VO<sub>2</sub> films produced by sol-gel spin coating on silica glass substrates, annealed at 450 °C for 15 minutes. The hysteresis plots were constructed at 2500 nm.



	nm) (%)	(cold)		(%)	(cold)	(hot)	
-	25	38.81	34.99	3.81	34.63	34.63	62
Na	41	39.16	29.71	9.44	38.55	36.10	57
K	31	37.55	32.12	5.43	37.33	36.87	47

#### 4. Conclusion Remarks

In summary, we investigated the behaviour of sodium and potassium doping on the thermochromic properties of the VO<sub>2</sub> thin films spin coated on silica and annealed at 450 °C. Both dopants, improved the  $\Delta T_{2500\text{ nm}}$  from 25 to 31 and 41 %; and  $\Delta T_{\text{sol}}$  to 9.44 and 5.43 % for sodium and potassium respectively. Both dopants lead to reduction of the transition temperature, K proved to be the more efficient than Na, exhibiting a  $T_c$  value of 47 °C, after 1.5 wt % dopant inclusion.

#### Acknowledgements

Işıl Top gratefully acknowledge Turkish Higher Research Council (TUBITAK) for PhD grant. Dr. Rory Wilson is thanked for his assistance with XRD for this work.

#### References

1. Kiria P, Hyett G, Binions R. Solid state thermochromic materials. *Adv Mater Lett.* 2010;1(2):86-105. doi:10.5185/amlett.2010.8147.
2. Ye H, Long L. Smart or not? A theoretical discussion on the smart regulation capacity of vanadium dioxide glazing. *Sol Energy Mater Sol Cells.* 2014;120:669-674. doi:10.1016/j.solmat.2013.10.018.
3. Kang M, Kim I, Kim SW, Ryu J-W, Park HY. Metal-insulator transition without structural phase transition in V2O5 film. *Appl Phys Lett.* 2011;98(13):131907. doi:10.1063/1.3571557.
4. Omer AM. Energy, environment and sustainable development. *Renew Sustain Energy Rev.* 2008;12:2265-2300. doi:10.1016/j.rser.2007.05.001.
5. Binions R, Piccirillo C, Palgrave RG, Parkin IP. Hybrid aerosol assisted and atmospheric pressure CVD of Gold-doped vanadium dioxide. *Chem Vap Depos.* 2008;14:33-39. doi:10.1002/cvde.200706641.
6. Narayan J, Bhosle VM. Phase transition and critical issues in structure-property correlations of vanadium oxide. *J Appl Phys.* 2006;100(10). doi:10.1063/1.2384798.
7. Michael E. A. Warwick RB. Advances in thermochromic vanadium dioxide film. *J Mater Chem A*,. 2014;2:3275.
8. Anderson A-L, Chen S, Romero L, Top I, Binions R. Thin Films for Advanced Glazing Applications. *Buildings.* 2016;6(3):37. doi:10.3390/buildings6030037.
9. Li SY, Niklasson GA, Granqvist CG. Nanothermochromics: Calculations for VO<sub>2</sub> nanoparticles in dielectric hosts show much improved luminous transmittance

and solar energy transmittance modulation. *J Appl Phys.* 2010;108(6). doi:10.1063/1.3487980.

10. Mlyuka NR, Niklasson G a., Granqvist CG. Thermochromic VO<sub>2</sub>-based multilayer films with enhanced luminous transmittance and solar modulation. *Phys Status Solidi Appl Mater Sci.* 2009;206(9):2155-2160. doi:10.1002/pssa.200881798.

11. Russell Binions, Ivan P. Parkin CP. Tungsten doped vanadium dioxide thin films prepared by atmospheric pressure chemical vapour deposition from vanadyl acetylacetonate and tungsten hexachloride. *Surf Coat Technol.* 2007;201:9369-9372.

12. Manning T, Parkin I, Blackman C, Qureshi U. APCVD of thermochromic vanadium dioxide thin films - solid solutions V<sub>2-x</sub>MxO<sub>2</sub> (M = Mo, Nb) or composites VO<sub>2</sub> : SnO<sub>2</sub>. 2005;2:4560-4566. doi:10.1039/b510552h.

13. Anderson A-L, Chen S, Romero L, Top I, Binions R. Thin Films for Advanced Glazing Applications. *Buildings.* 2016;6(3):37. doi:10.3390/buildings6030037.

14. Manning T, Parkin I. Atmospheric pressure chemical vapour deposition of tungsten doped vanadium(IV) oxide from VOCl<sub>3</sub>, water and WCl<sub>6</sub>. *J Mater.* 2004;14:2554-2559. doi:10.1039/b403576n.

15. Piccirillo C, Binions R, Parkin IP. Synthesis and characterisation of W-doped VO<sub>2</sub> by Aerosol Assisted Chemical Vapour Deposition. *Thin Solid Films.* 2008;516(8):1992-1997. doi:10.1016/j.tsf.2007.06.009.

16. Zhao L, Miao L, Tanemura S, et al. A low cost preparation of VO<sub>2</sub> thin films with improved thermochromic properties from a solution-based process. *Thin Solid Films.* 2013;543:157-161. doi:10.1016/j.tsf.2012.11.154.

17. Batista C, Ribeiro RM, Teixeira V. Synthesis and characterization of VO<sub>2</sub>-based thermochromic thin films for energy-efficient windows. *Nanoscale Res Lett*. 2011;6(1):301. doi:10.1186/1556-276X-6-301.
18. Hanlon TJ, Coath JA, Richardson MA. Molybdenum-doped vanadium dioxide coatings on glass produced by the aqueous sol-gel method. *Thin Solid Films*. 2003;436(03):269-272. doi:10.1016/S0040-6090(03)00602-3.
19. Mai LQ, Hu B, Hu T, Chen W, Gu ED. Electrical property of Mo-doped VO<sub>2</sub> nanowire array film by melting-quenching sol-gel method. *J Phys Chem B*. 2006;110(39):19083-19086. doi:10.1021/jp0642701.
20. Dai L, Chen S, Liu J, et al. F-doped VO<sub>2</sub> nanoparticles for thermochromic energy-saving foils with modified color and enhanced solar-heat shielding ability. *Phys Chem Chem Phys*. 2013;15(28):11723-11729. doi:10.1039/c3cp51359a.
21. Mlyuka NR, Niklasson G a., Granqvist CG. Mg doping of thermochromic VO<sub>2</sub> films enhances the optical transmittance and decreases the metal-insulator transition temperature. *Appl Phys Lett*. 2009;95(17):2-4. doi:10.1063/1.3229949.
22. Song L, Zhang Y, Huang W, et al. Preparation and thermochromic properties of Ce-doped VO<sub>2</sub> films. *Mater Res Bull*. 2013;48:2268-2271. doi:10.1016/j.materresbull.2013.02.016.
23. Dietrich MK, Kramm BG, Becker M, Meyer BK, Polity A, Klar PJ. Influence of doping with alkaline earth metals on the optical properties of thermochromic VO<sub>2</sub>. *J Appl Phys*. 2015;117(18). doi:10.1063/1.4919433.
24. Zhang J, He H, Xie Y, Pan B. Giant Reduction of the Phase Transition Temperature for Beryllium Doped VO<sub>2</sub>. *Phys Chem Chem Phys*. 2013;15(13):4687-

4690. doi:10.1039/c3cp44476g.

25. Song Q, Gong W, Ning G, et al. A synergic effect of sodium on the phase transition of tungsten-doped vanadium dioxide. *Phys Chem Chem Phys*. 2014;16(19):8783-8786. doi:10.1039/c4cp00366g.

26. Cui Y, Wang Y, Liu B, et al. First-principles study on the phase transition temperature of X-doped (X = Li, Na or K) VO<sub>2</sub>. *RSC Adv*. 2016;6(69):64394-64399. doi:10.1039/C6RA10221B.

27. Vroon ZAEP, Spee CIMA. Sol—gel coatings on large area glass sheets for electrochromic devices. *J Non Cryst Solids*. 1997;218:189-195. doi:10.1016/S0022-3093(97)00275-5.

28. Wu J, Huang W, Shi Q, et al. Effect of annealing temperature on thermochromic properties of vanadium dioxide thin films deposited by organic sol–gel method. *Appl Surf Sci*. 2013;268:556-560. doi:10.1016/j.apsusc.2013.01.007.

29. Strelcov E, Tselev A, Ivanov I, et al. Doping-based stabilization of the M2 phase in free-standing VO<sub>2</sub> nanostructures at room temperature. *Nano Lett*. 2012;12(12):6198-6205. doi:10.1021/nl303065h.

30. Cao C, Gao Y, Luo H. Pure Single-Crystal Rutile Vanadium Dioxide Powders: Synthesis, Mechanism and Phase-Transformation Property. 2008:18810-18814. doi:10.1021/jp8073688.

31. Silversmit G, Depla D, Poelman H, Marin GB, De Gryse R. Determination of the V2p XPS binding energies for different vanadium oxidation states (V<sup>5+</sup> to V<sup>0+</sup>). *J Electron Spectros Relat Phenomena*. 2004;135(2-3):167-175. doi:10.1016/j.elspec.2004.03.004.

32. Hu L, Tao H, Chen G, et al. Porous W-doped VO<sub>2</sub> films with simultaneously enhanced visible transparency and thermochromic properties. *J Sol-Gel Sci Technol.* 2016;77(1):85-93. doi:10.1007/s10971-015-3832-z.

33. Sun Y, Xiao X, Xu G, et al. Anisotropic vanadium dioxide sculptured thin films with superior thermochromic properties. *Sci Rep.* 2013;3(1):2756. doi:10.1038/srep02756.

34. Zhang Z, Gao Y, Chen Z, et al. Thermochromic VO<sub>2</sub> thin films: Solution-based processing, improved optical properties, and lowered phase transformation temperature. *Langmuir.* 2010;26(13):10738-10744. doi:10.1021/la100515k.

35. Liang Z, Zhao L, Meng W, et al. Tungsten-doped vanadium dioxide thin films as smart windows with self-cleaning and energy-saving functions. *J Alloys Compd.* 2017;694:124-131. doi:10.1016/j.jallcom.2016.09.315.